Green Chemistry

Accepted Manuscript

ROYAL SOCIETY OF CHEMISTRY

www.rsc.org/greenchem

Preparation of $CuCr_2O_4$ Spinel Nanoparticles Catalyst for Selective Oxidation of Toluene to Benzaldehyde†

Shankha Shubhra Acharyya,[a] Shilpi Ghosh,[a] Ritesh Tiwari,[a] Bipul Sarkar,[a] Rajib Kumar Singha[a], Chandrasekar Pendem,[a] Takehiko Sasaki[b] and Rajaram Bal*[a]

[a]*Catalytic Conversion & Processes Division, CSIR-Indian Institute of Petroleum, Dehradun 248005, India*

[b]*Department of Complexity Science and Engineering, Graduate School of Frontier Sciences, The University of Tokyo, Kashiwanoha, Kashiwa-shi, Chiba 277-8561, Japan*

[*] Mr. Shankha Shubhra Acharyya, Ms. Shilpi Ghosh, Mr. Ritesh Tiwari, Mr. Bipul Sarkar, Mr. Rajib Kumar Singha, Mr. Chandrashekar Pendem, Prof. Dr. Takehiko Sasaki, Dr. Rajaram Bal

Corresponding author. Tel.: +91 135 2525797; Fax: +91 135 2660202

E-mail addresses: raja@iip.res.in

$CuCr_2O_4$ spinel nanoparticles with the size between 30-60 nm was prepared by a hydrothermal synthesis method in the presence of surfactant, cetyltrimethylammonium bromide (CTAB). It was found that the catalyst is highly active for the selective oxidation of toluene with H_2O_2 at 75° C. The catalyst was characterized by XRD, ICP-AES, XPS, TPR, BET-surface area, SEM, TEM and EXAFS. Factors effecting reaction parameters, such as the substrate to oxidant molar ratio, weight of catalyst, reaction time, etc. were investigated in detail. The investigation revealed that the size of the catalyst as well as the spinel phase plays a crucial role towards the activity by favoring the oxidation of toluene. The reusability of the catalyst was examined by conducting repeat experiments with the same catalyst; and it was observed that the catalyst displayed no significant changes in its activity even after 5 reuses. The toluene conversion of 57.5 % with 84.4% selectivity towards benzaldehyde was observed after 10 hours over $CuCr_2O_4$ spinel nanoparticles catalyst.

1. Introduction

Controlled synthesis of inorganic nanoparticles is of both fundamental and technical interest due to their size and shape dependent physical properties and diverse applications. The simple preparation method is required for easy manipulation of the nucleation and growth kinetics for tunable shape and size of the nanoparticles.[1,2] Bimetallic nanoparticles (NP), emerging as a new class of materials, are of much potential interest compared to the monometallic ones as they generate new properties and capabilities due to a synergy between the two metals.[3,4] Moreover, bimetallic NPs usually show composition-dependent surface structure and atomic segregation behavior, and thus bear attracted attention in multidisciplinary fields. Compared to the monometallic NPs, synthesis of high-quality bimetallic ones with controllable size, morphology, composition, and structure is much more complicated; therefore, a simple, reliable preparation is still remains a challenge to be solved.[5,6] Copper chromium mixed oxides with a spinel structure are an important class of bi- metallic oxides promise great potentials as versatile catalyst and thus, bears wide commercial applications.[7-9] These catalysts can be prepared by a variety of synthetic methods.[7,10,11] Among these methods, the sol-gel process using metal alkoxide shows promising potential, owing to its high purity, good chemical homogeneity etc. but suffers due to its sensitivity towards moisture and heat.[12] So, controlled syntheses of copper chromite at large scale, with tunable morphology and its fruitful application in catalytic oxidation is highly appreciated in the field of catalysis.

Herein, we report for the first time the preparation of $CuCr_2O_4$ spinel nanoparticles by hydrothermal synthesis method. This preparation method is simple, reproducible and produces high yield (98%) and can be prepared in a large scale (upto 20 g). To the best of our knowledge, there is no report for the preparation of $CuCr_2O_4$ spinel nanoparticles with size between 20-40 nm using surfactant promoted hydrothermal synthesis method.

Direct functionalization of sp^3 hybridized inactive hydrocarbons by means of catalytic oxidation of C-H bonds to form oxygenated products under mild conditions is a major challenge from industrial aspects.[13,14] Toluene is a typical aromatic hydrocarbon, that possesses three primary C-H bonds and can be oxidized to several oxygenates like benzyl alcohol, benzaldehyde, benzoic acid, and benzoate, which are all useful chemical intermediates.[15] Among these, benzaldehyde is the most desirable product due to its immense importance in our daily life.[16] It is used in the manufacture of dyes, solvents, perfumes, flavors, plasticizers, dyestuffs, preservatives and flame retardants. In the pharmaceutical industries, it is used for the manufacture of intermediates for chloramphenicol, analgin, ephidrin, ampiphilicin etc. Traditionally, benzaldehyde is produced by chlorination of $–CH_3$ functionality of toluene followed by saponification.[17] These processes suffer severely from much waste causing environmental problems and poor efficiencies. Moreover, the products are not prescribable for edible and drug grade specifications owing to the chlorinated contaminants. Although, there are some reports on vapor phase oxidation of toluene with oxygen, but the conducting reaction conditions are harsh and the selectivity are not satisfactory.[18-20] Although, in the Rhodia, Dow and Snia-Viscosa processes liquid phase oxidation of toluene is carried out over homogeneous metal salt catalysts using oxygen or peroxides as oxidants in industrial grade, involved indispensable halogen ions and acidic solvents cause corrosion of the facility.[21-23] There are also several reports using H_2O_2[24], TBHP[25] and molecular O_2 as oxidant for oxidation of toluene to benzaldehyde but most of the cases yield is very less.[21,26-28] Apart from these, there are also few reports on selective oxidation of toluene to benzaldehyde using photocatalytic routes.[29,30] Recently, Antonietti and his group reported toluene oxidation using B-doped polymeric carbon nitride (graphitic phase) with H_2O_2 as oxidant[31] and using mesoporous nano-structured carbon nitride with O_2 as oxidant.[32] Although, they reported a high selectivity towards benzaldehyde (~99%), but the conversion of toluene was very poor.

Herein we report the unique catalytic activity of our so prepared $CuCr_2O_4$ spinel nanoparticles in selective oxidation of toluene to benzaldehyde. A toluene conversion of 57.5 % and 84.4% benzaldehyde selectivity was achieved with H_2O_2 as the principal oxygen donor at 75°C in liquid phase.

2. Experimental

2.1 Material

Hydrogen Peroxide (50 wt % in water) was purchased from Merck KGaA, Darmstadt, Germany. $Cu(NO_3)_2 \cdot 5H_2O$, $Cr(NO_3)_3 \cdot 9H_2O$, cetyltrimethylammonium bromide, hydrazine, ammonium hydroxide, toluene (purity > 99.9%), acetonitrile (HPLC grade) were purchased from Sigma-Aldrich Co. All the chemicals were used without further purification.

2.2 Catalyst Preparation

The $CuCr_2O_4$ spinel nanoparticles catalyst was prepared hydrothermally using cetyltrimethylammonium bromide as the surfactant by modifying our own preparation method.[33] An aqueous solution of 3.8 g Cu $(NO_3)_2.3H_2O$ was added with vigorous stirring to 12.6 g Cr $(NO_3)_3.9H_2O$ dissolved in 80 g deionized water. The pH of the medium was made 9 by adding drop wise ammonia solution. An aqueous solution of 4.3 g CTAB, followed by of 0.98 g hydrazine was added drop wise to the reaction mixture. The reagents were added maintaining the molar ratio: Cu: Cr: CTAB: H_2O: hydrazine = 1: 2: 0.75: 300: 1. After stirring, the so obtained homogeneous solution was hydrothermally treated at 180 °C for 24 h in a teflon-lined autoclave vessel under autogeneous pressure. The product was washed with distilled water, acetone and ethanol and dried at 110 °C, for 10 h, followed by calcination at 650 °C for 6 h in air.

2.3 Catalyst Characterization

Powder X-ray diffraction (XRD) Powder X-ray diffraction (XRD) patterns were collected on a Bruker D8 advance X-ray diffractometer fitted with a Lynx eye high-speed strip detector and a Cu K_α radiation source. Diffraction patterns in the 2º-80º region were recorded at a rate of 0.5 degrees (2q) per minute. Scanning electron microscopy (SEM) images were taken on a FEI

Quanta 200 F, using tungsten filament doped with lanthanumhexaboride (LaB_6) as an X-ray source, fitted with an ETD detector with high vacuum mode using secondary electrons and an acceleration tension of 10 or 30 kV. Samples were analyzed by spreading them on a carbon tape. Energy dispersive X-ray spectroscopy (EDX) was used in connection with SEM for the elemental analysis. The elemental mapping was also collected with the same spectrophotometer. Transmission electron microscopy (TEM) images were collected using a JEOL JEM 2100 microscope, and samples were prepared by mounting an ethanol-dispersed sample on a lacey carbon Formvar coated Cu grid. The surface area was measured using Belsorp equipment (BEL Japan Inc.) by nitrogen adsorption at -196 ºC. Prior to measurement, the sample was pretreated at 200 ºC for 3 h under vacuum. X-Ray photoelectron spectra were recorded on a Thermo Scientific K-Alpha X-Ray photoelectron spectrometer and binding energies (±0.1 eV) were determined with respect to the position C 1s peak at 284.8 eV. Extended X-ray absorption fine structure spectroscopy (EXAFS) measurements of Cu-K edge were carried out at the High Energy Accelerator Research Organization (KEK-IMMS-PF), Tsukuba, Japan. The measurement was made at transition mode and spectra were taken at BL-7C and BL-9C. The electron storage ring was operated at 2.5 GeV and 450 mA, synchrotron radiation from the storage ring was monochromatized by a Si (111) channel cut crystal. Ionized chamber, which were used as detectors for incident X-ray (I_o) and transmitted X-ray (I), were filled with N_2 mixture gas, respectively. The angle of the monochromators was calibrated with Cu foil. The EXAFS raw data were analyzed with UWXAFS analysis package including background subtraction program AUTOBK and curve fitting program FEFFIT.[34-36] The amplitude reducing factor, S_o^2 was fixed at 1.0. The backscattering amplitude and phase shift were calculated theoretically by FEFF 8.4 code.[37] ATOMS were used to obtain FEFF input code for crystalline materials.[38] Inductively coupled Plasma Atomic Emission Spectroscopic (ICP-AES) analysis was carried out by Inductively Coupled Plasma Atomic Emission Spectrometer; model: PS 3000 uv, (DRE), Leeman Labs, Inc, (USA). Thermogravimetric Analysis (TGA) and Differential Thermal Analysis (DTA) of the uncalcined catalyst were carried out in a PYRIS DIAMOND, PERKIN ELMER INSTRUMENTS. 2.15 mg samples was used and a heating rate of 5 °C min^{-1} was carried out in flowing air. The FTIR spectra were recorded on a Thermo Nicolet 8700 (USA) instrument with the operating conditions: resolution: 4 cm^{-1}, scan: 36, operating temperature: 23-25 °C and the frequency range: 4000-400cm^{-1}.

2.4 Oxidation of toluene

Liquid phase oxidation reaction was carried out in a two neck round bottom flask containing 0.1 g catalyst, 15 ml solvent and 1 g toluene to which H_2O_2 (50% aq. solution) was added dropwise. Small aliquots of the sample were withdrawn from the reaction mixture at regular intervals for analysis using a syringe. At the end of the reaction, the solid particles (catalyst) were separated by filtration and the products were analysed by Gas Chromatography (GC, Agilent 7890) connected with a HP5 capillary column (30m length, 0.28 mm id, 0.25 µm film thickness) and flame ionisation detector (FID). The toluene conversion and benzaldehyde formation were calculated using a calibration curve (obtained by manual injecting the authentic standard compounds). The individual yields were calculated and normalized with respect to the GC response factors. The product identification was carried out by injecting the authentic standard samples in GC and GC-MS. The C-balance as well as material balance was carried out for most of the experiments and it was found between 98-102%. After completion of the reaction, the catalyst was recovered from the reaction mixture via centrifugation, washed thoroughly with acetone and reused for multiple circles.

3. Results and discussion

3.1 Catalyst Characterization

The powder XRD pattern of the prepared Cu-Cr catalyst (Fig. 1) revealed the exclusive formation of $CuCr_2O_4$ spinel with high phase-crystallinity (JCPDS Card No: 05-0657), while no XRD peaks were attributed either to Cu or Cr metal, or their oxides. The particle size was determined from the full width half maxima of the line broadening corresponding to the diffraction angle of 53.4° by using the Scherrer equation and a mean particle size of ~28 nm was observed (Table 1). The amount of copper and chromium present in the sample was estimated by ICP-AES and it was found that the molar ratio of Cu to Cr was 0.5, which is the typical composition of $CuCr_2O_4$ spinel. The catalyst was stable above 1000°C as confirmed by TG/DTA analysis (Fig. S1 & S2, ESI).

SEM image (Fig. 2) showed the formation of almost homogeneously distributed uniform particles with size 20-40 nm. Energy dispersive X-Ray analysis (EDAX) showed the presence of Cu, Cr, O (Fig. 3) and the elemental mapping demonstrated the homogeneous distribution of Cu and Cr in the catalyst (Fig. 4).

Transmission Electron Microscopy (TEM) images of the $CuCr_2O_4$ spinel catalyst are shown in Fig. 5. The particle size distribution histogram is also presented in Fig. 5a (inset). The distribution histogram shows that 10% particles have the diameter of 20 nm, 38% particles have the diameter of 30 nm, 26% particles have the diameter of 40 nm, 10% particles have diameters of 50 nm and rest of the particles (16%) having diameter more than 50 nm. The lattice fringes with a d-spacing of 0.30 nm corresponding to [220] plane of $CuCr_2O_4$ spinel[39] with diffraction angle (2θ) of 29.6 is also presented. The HRTEM of the spent catalyst (after 5 recycle)(Fig. 5d) revealed that the particle size of the $CuCr_2O_4$ spinel was unchanged during the catalysis.

The Cu_{2p} XPS spectrum of the fresh catalyst is characterized by two spin-orbit doublets with strong satellite peaks which are of typical Cu^{2+} (Fig. 6). The low energy component with $Cu_{2p3/2}$ at 933.8 eV is associated to Cu^{2+} in octahedral sites, whereas the high energy component at 935.2 eV is associated with Cu^{2+} in the tetrahedral sites of the $CuCr_2O_4$ spinel structure. The $Cr_{2p\ 3/2}$ core level spectra of the $CuCr_2O_4$ fresh catalyst appeared at 576.5 eV showed the presence of Cr^{3+} ions and the O_{1s} binding energies appeared at 530.2 eV and 532.2 eV, revealed the presence of O^{2-} species in $CuCr_2O_4$ spinel (Fig. S3 & S4, ESI).[40]

Cu-K edge extended X-ray absorption fine structure (EXAFS) analysis of the catalyst supports the formation of $CuCr_2O_4$ spinel and the spinel structure remains unchanged during the catalysis (Table 2 & Fig. S5, ESI). The entry for CuO is not for the reference compound. The EXAFS spectrum was analyzed as the superposition of the crystal phase of $CuCr_2O_4$ and the residual CuO phase. The small coordination number 2.5 for the CuO phase indicates that the CuO phase correspond to the surface layer of oxidized Cu on $CuCr_2O_4$ crystal or the monatomically dispersed CuO on the $CuCr_2O_4$ crystal phase. From Cu2p XPS spectra, tetrahedrally coordinated Cu and the octahedrally coordinated Cu are assigned to the $CuCr_2O_4$ phase and the surface CuO phase, respectively. The coordination number for CuO was found to be smaller than the value 4-6 in the present study, because it is minor phase as compared to the $CuCr_2O_4$ phase.

It is worth mentioning that, the embedment of the CTAB molecules can be analyzed by the FTIR analysis (Fig. 7). A comparison of the FTIR- spectra of dried uncalcined sample, with that of pure CTAB was analyzed, which not only confirmed the presence, but also revealed the nature of interaction of CTA- molecules with the Cu-Cr surface. The peaks of the sample at 809, 1062 cm^{-1} can be assigned to the C-N^+ stretching modes of CTAB molecules.[41] The peak at 1378 and at 1462 cm^{-1} were assigned to symmetric mode of vibration of the head groups of the methylene moiety (N^+—CH_3) and CH_2 scissoring mode respectively.[41] The frequencies above 1600 cm^{-1} to 3000 cm^{-1} can be attributed due to CH_2 symmetric antisymmetric vibrations region. It is to be noted that, the shift of vibrations to lower frequency suggested that, alkyl chains experienced a more hydrophobic environment in Cu-Cr blocks upon the surface of which the CTAB moieties were supposed to be bounded.[41] These typical frequencies were absent when the material was calcined at 650 °C in air (fresh catalyst)in the case of the prepared catalyst, which indicated that, the embedded CTAB moieties have been completely removed from the catalyst surface during calcination. Moreover, in the SEM-EDAX diagram of the fresh catalyst (Fig. 3) does not show any peak for C, N or even Br, which further ascertains the removal of the template (CTAB) by calcination.

Based on these detailed characterization data, we presented a model diagram of $CuCr_2O_4$ spinel catalyst (Fig. S6, ESI), which actually reflects the three-dimensional array of Cu, Cr and O atoms in the catalyst.

3.2 Activity of the catalyst

Table 3 shows the activities of the $CuCr_2O_4$ spinel nanoparticles catalyst in the direct oxidation of toluene in liquid phase by using H_2O_2 as oxidant. The catalyst shows 57.5% toluene conversion with 84.4% selectivity of benzaldehyde. The remaining major product was benzylalcohol with 11.2% selectivity. So a total C7 (benzaldehyde and benzylalcohol) selectivity of 95.6% was achieved over this catalyst. Blank experiment was carried out without the catalyst and it was found that there was no conversion of toluene. For comparison several different Cu supported catalysts were prepared and their activity was tested for toluene oxidation. Commercial CuO, Cu_2O, Cr_2O_3 does not show any activity for toluene oxidation (Table 3, entry 1-3). Although, commercial $CuCr_2O_4$, Cu-supported on commercial Cr_2O_3, prepared impregnation method and co-precipitation method show some selectivity for benzaldehyde with negligible activity but the catalysts show serious leaching, as confirmed by ICP-AES (Table 3, entry 4-6). We have also tested the catalytic activity of the Cu-nanoclusters supported on nanocrystalline Cr_2O_3 and noticed that this catalyst shows 12.5 % conversion and 65.2% benzaldehyde selectivity (entry 7). Although this catalyst shows good benzaldehyde selectivity but this catalyst shows leaching of Cu during reaction. This result clearly indicates that spinel phase ($CuCr_2O_4$) and small Cu^{2+} site are essential for selective oxidation of toluene to benzaldehyde.

3.3 Effect of reaction parameters

It was found that temperature has prominent effect on toluene conversion. The catalyst showed negligible conversion at RT but with increasing temperature, the conversion of toluene increases rapidly (Fig. 8). Presence of both benzyl alcohol and benzaldehyde exclusively was noticed in the reaction mixture; moreover at 75 °C, low concentration of H_2O_2 and low catalyst weight facilitates the formation of benzyl alcohol on the catalyst surface; but with the increase in temperature, time and H_2O_2 concentration, conversion of benzyl alcohol to benzaldehyde occurs, thereby selectivity of the latter increases significantly. The observed decrease in selectivity was due to the formation of *para*- and *ortho*-isomer of cresols and over-oxidized product, benzoic acid. It was also found that, the catalyst was active only in acetonitrile solvent Increment in H_2O_2 molar ratio allows oxidation of the side chain and in the aromatic system, both and consequently the concentration of the side products increases (Fig. 10). Increment in time and temperature both indicates the fact that, the species present in the reaction mixture are allowed to react without excess oxidant; inevitably, concentration of benzoic acid (a stable oxidation product) owing to autooxidation of benzaldehyde (and benzyl alcohol) occurs. It seems, acetonitrile (solvent) activates H_2O_2 by forming a perhydroxyl anion (HOO^-, nucleophile)[42] which attacks the C—N group of the acetonitrile to generate peroxycarboximidic acid intermediate, a good oxygen transfer agent,[43] and thereby explains the solvent efficacy in the reaction. Moreover, conducting the reaction in different solvents did not show any satisfactory yields. It seems that polarity of the solvent does not play significant effect in this reaction. The conversion of toluene was extremely poor in DMF and ^{n}octane; although selectivity of benzaldehyde was ~98% in acetic acid, conversion was very low.

3.5 Reusablity of the catalyst

The catalyst displayed a high-leaching resistance capability. Reuse of the recovered catalyst in 5 consecutive runs did not lead to any significant decline in its catalytic activity in terms of conversion, yield and selectivity. Recycling and reusability of the catalyst was examined by introducing the used catalyst subsequently 5 times to carry out the catalytic oxidation reaction unhindering the optimum conditions; After the first reaction cycles (10 h), the solid catalyst was recovered by a centrifugation and washed with acetone and dried for the next reaction cycle. The catalyst was effective enough in each cycle (Fig. 12), which demonstrates that, no structural modification, like sintering could have hardly hampered the spinel phase and no significant loss in the catalytic activity was observed; hence recovered catalyst could be reused several times, establishing the recyclability of the catalyst. Moreover, to examine the heterogeneous nature, we tested the activity of the filtration. When a typical oxidation of toluene was proceeded for 5h (when 40% toluene conversion was achieved) the reaction was stopped and the filtrate was immediately collected. No further increase in conversion was observed after the filtrate was stirred at 75° C for another 5h. These results clearly indicate that the conversion was contributed exclusively by $CuCr_2O_4$ spinel NP catalyst and leaching of the catalyst hardly occurred during the reaction, which was furthermore ascertained by ICP-AES analyses and XRD plot of the catalyst during the recycling experiments.

4 Conclusions

We have prepared $CuCr_2O_4$ spinel nano particles with size between 30-60 nm by hydrothermal synthesis method in presence of surfactant. This catalyst can efficiently catalyze the oxidation of toluene through intervening the activation of C–H bonds, and can operate under mild conditions and can generate selectively benzyl alcohol and benzaldehyde, tuning the reaction parameters inconveniently, currently remain to be the major research effort in catalysis. The catalyst can be reused several times without any activity loss, confirming the true heterogeneous nature of the catalyst.

Acknowledgements

The Director, CSIR-IIP, is acknowledged for his help and encouragement. S.S.A. thanks CSIR and S.G., B.S., R.K.S. thank UGC, New Delhi, India for their fellowships. The authors thank Analytical Science Division, Indian Institute of Petroleum for analytical services. The XAFS measurements were performed at KEK-IMSS-PF, Tsukuba, Japan with the approval of the Photon Factory Advisory Committee (project 2010G109).

Notes and References:

1. S. Wu, G. Han, D. J. Milliron, S. Aloni, V. Altoe, D. V. Talapin, B. E. Cohen and P. J. Schuck, *Proc. Natl. Acad. Sci.*, 2009, **106**, 10917.
2. J. Zhuang, A. D. Shaller, J. Lynch, H. Wu, O. Chen, A. D. Q. Li and Y. C. Cao, *J. Am. Chem. Soc.*, 2009, **131**, 6084.
3. M. Jaime, R. Movshovich, G. R. Stewart, W. P. Beyermann, M. G. Berisso, M. F. Hundley, P. C. Canfield and J. L. Sarrao, *Nature,* 2000, **405**, 160.
4. D. Xu, Z. P. Liu, H. Z. Yang, Q. S. Liu, J. Zhang, J. Y. Fang, S. Z. Zou and K. Sun, *Angew. Chem. Int. Ed.,* 2009, **48**, 4217.
5. U. Banin, *Nature Mater.,* 2007, **6**, 625.
6. D. Wang and Y. Li, *Adv. Mater.,* 2011, **23**, 1044.
7. R. Connor, K. Folker and H. Adkins, *J. Am .Chem. Soc*., 1931, **53**, 2012.
8. R. Prasad and P. Singh, *Catal. Rev. Sci.& Eng.,* 2012, **54***,* 224.
9. K. L. Deutsch and B. H. Shanks, *J. Catal*., 2012, **285**, 235.
10. T. Valde´s-Soli´s, G. Marba´n and A. B. Fuertes, *Chem. Mater.,* 2005, **17***,* 1919.
11. Y. Tanaka, T. Takeguchi, R. Kikuchi and K. Eguchi, *Appl. Catal. A,* 2005, **279**, 59.
12. L. Castro, *J. Sol-Gel Sci. Technol.,* 2002, **25**, 159.
13. R. A. Sheldon and H. van Bekkum, *Fine Chemicals through Heterogeneous Catalysis,* Wiley-VCH, Weinheim, 2001, 1.
14. J. M. Thomas, R. Raja, G. Sankar and R. G. Bell, *Nature,* 1999, **398**, 227.

15. L. Kesavan, D. I. Enache, S. H. Taylor, R. Tiruvalam, R. L. Jenkins, D. W. Knight, M. H. A. Rahim, N. Dimitratos, C. J. Kiely, M. I. bin Saiman, J. A. Lopez-Sanchez and G. J. Hutchings, *Science,* 2011, **331**, 195.

16. F. Bruhne and E. Wright, *Ullmann's Encyclopedia of Industrial Chemistry*, Wiley-VCH, Weinheim, 2012, **5**, 223.

17. W. Partenheimer, *Catal. Today,* 1995, **23**, 69.

18. C. Subrahmanyam, B. Louis, F. Rainone, B. Viswanathan, A. Renken and T. K. Varadarajan, *Catal. Commun.,* 2002, **3**, 45.

19. A. Martin, U. Bentrup and G. U. Wolf, *Appl. Catal. A*, 2002, **227**, 131.

20. C. C. Guo, Q. Liu, X. T. Wang, H. Y. Hu, *Appl. Catal. A*, 2005, **282**, 55.

21. F. Wang, J. Xu, X. Q. Li, J. Gao, L. P. Zhou and R. Ohnishi, *Adv. Synth. Catal.* 2005, **347**, 1987.

22. T. Garrell, S. Cohen and G. C. Dismukes, *J. Mol. Catal. A,* 2002, **187**, 3.

23. Snia-Viscosa, *Hydrocarbon Proc.,* 1977, **134**, 210.

24. X. Wang, J. Wu, M. Zhao, Y. Lv, G. Li and C. Hu, *J. Phys. Chem. C*, 2009, **113**, 14270.

25. M. I. bin Saiman, G. L. Brett, R. Tiruvalam, M. M. Forde, K. Sharples, A. Thetford, R. L. Jenkins, N. Dimitratos, J. A. Lopez-Sanchez, D. M. Murphy, D. Bethell, D. J. Willock, S. H. Taylor, D. W. Knight, C. J. Kiely and G. J. Hutchings, *Angew. Chem. Int. Ed.,* 2012, **51**, 5981.

26. M. L. Kantam, P. Sreekanth, K. K. Rao, T. P. Kumar, B. P. C. Rao and B. M. Choudary, *Catal Lett*., 2002, **81**, 223.

27. J. Lv, Yi Shen, L. Peng, X. Guo and W. Ding, *Chem. Commun.,* 2010, **46**, 5909.

28. Y. Luo and D. F. Ollis, *J. Catal*, 1996, **163,** 1.

29. Y. Mao and A. Bakac, *J. Phys. Chem.,* 1996, **100**, 4219.

30. H. Lin, J. Long, Q. Gu, W. Zhang, R. Ruan, Z. Li and X. Wang, *Phys. Chem. Chem. Phys.,* 2012, **14**, 9468.

31. Y. Wang, H. R. Li, J. Yao, X. C. Wang and M. Antonietti, *Chem. Sci.,* 2011, **2**, 446.

32. X. H. Li, X. Wang and M. Antonietti, *ACS Catal.,* 2012, **2**, 2082.

33. B. Sarkar, P. Prajapati, R. Tiwari, R. Tiwari, S. Ghosh, S. S. Acharyya, C. Pendem, R. K. Singha, L. N. S. Konathala, J. Kumar, T. Sasaki and R. Bal, *Green Chem.,* 2012, **14**, 2600.

34. E. A. Stern, M. Newville, B. Ravel, Y. Yacoby and D. Haskel, *Physica B,* 1995, **117**, 208.

35. M. Newville, P. Livins, Y. Yacoby, E. A. Stern and J. J. Rehr, *Phys. Rev. B,* 1995, **47**,14126.

36. A. L. Ankudinov, B. Ravel, J. J. Rehr and S. D. Conradson, *Phys. Rev. B,* 1998, **58**, 7565.

37. A. L. Ankudinov, A. I. Nesvizhskii, and J. J. Rehr, *Phys. Rev. B,* 2003, **67**, 115120.

38. B. Ravel, *J. Synchrotron Rad.,* 2001, **8**, 314.

39. A. M. Kawamoto, L. C. Pardini and L. C. Rezende, *Aerosp. Sci. Technol.,* 2004, **8**, 591.

40. F. Severino, J. L. Brito, J. Laine, J. L. G. Fierro and A. Lo´pez Agudoy, *J. Catal.,* 1998, **177**, 82.

41. W. Cheng, S. Dong and E. Wang, *Langmuir,* 2003, **19,** 9434.

42. G. V. Nizova, Y. N. Kozlov and G. B. Shulpin, *Russ. Chem. Bull. Int. Ed.,* 2004, **53**, 2330.

43. U. R. Pillai and E. Sahle-Demessie, *New J. Chem.,* 2003, **27**, 525.

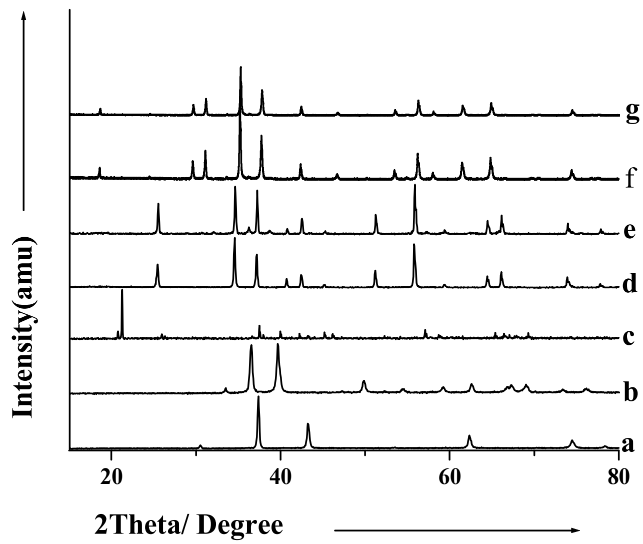

Fig. 1 XRD patterns of the a) CuO, b) Cu_2O, c) CrO_3, d) Cr_2O_3, e) $Cu/Cr_2O_3^{imp}$ (imp: impregnation method), f) $CuCr_2O_4$ (prepared catalyst) and g) $CuCr_2O_4$ (spent catalyst, after 5 reuse).

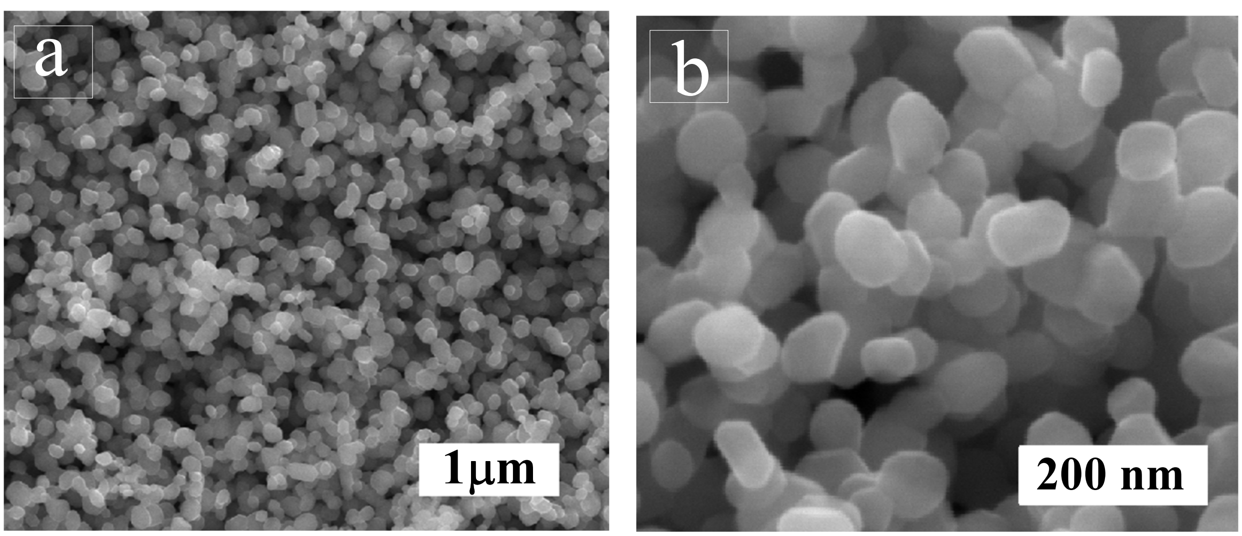

Fig. 2 SEM image of $CuCr_2O_4$ nanoparticles: a) low magnification and b) high magnification

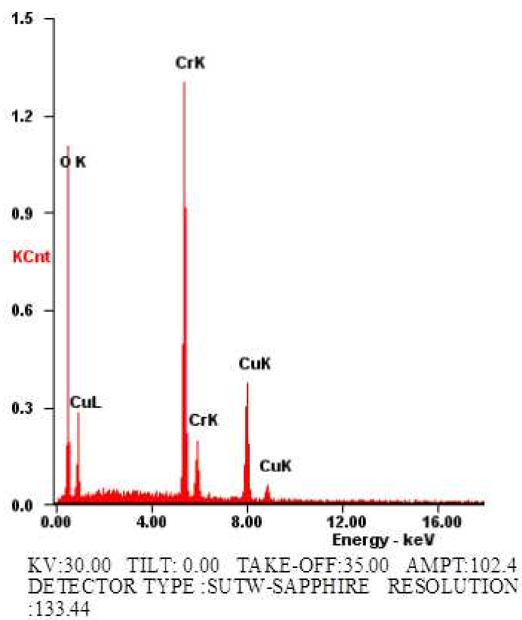

Fig. 3 SEM-EDAX spectra of $CuCr_2O_4$ spinel nanoparticles catalyst.

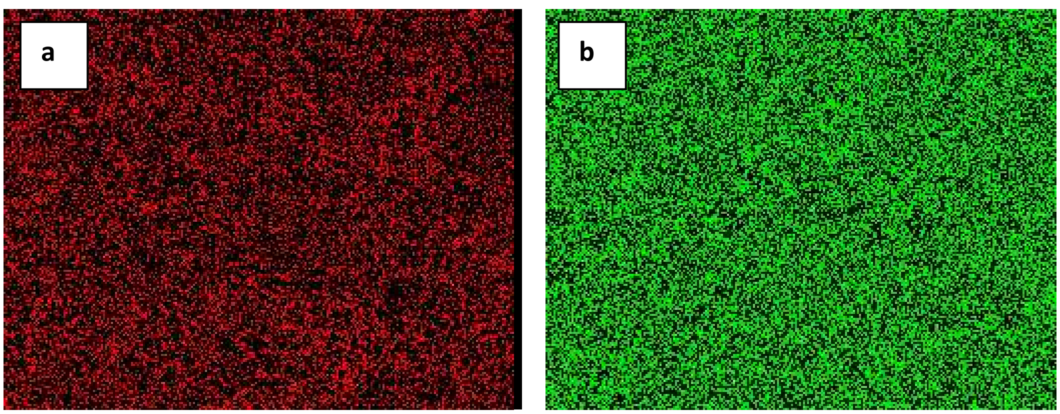

Fig. 4 Elemental Mapping of a) Cu atoms and b) Cr atoms in $CuCr_2O_4$ spinel nanoparticles catalyst.

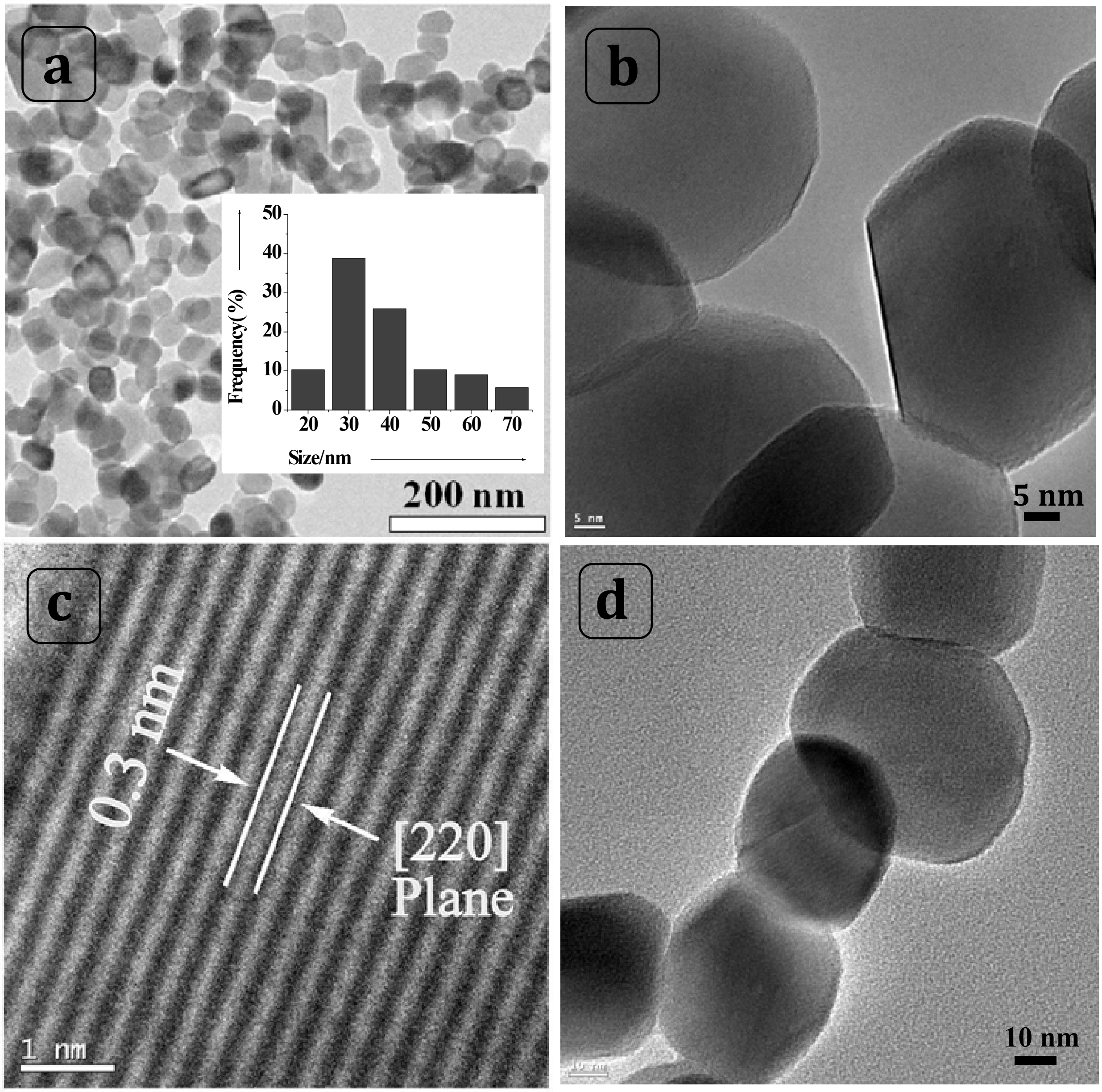

Fig. 5 TEM images of a) - c) fresh and d) spent catalyst.

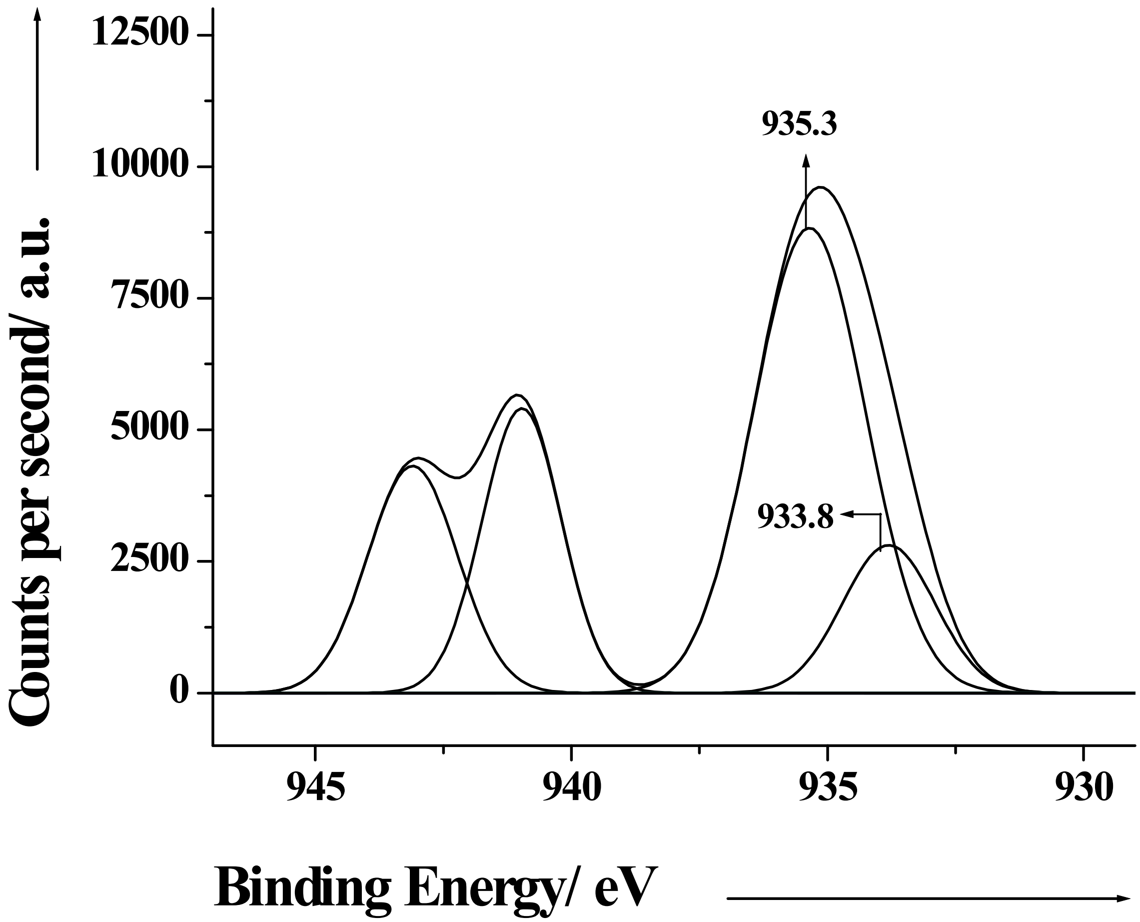

Fig. 6 Cu 2p $_{3/2}$ core level spectra

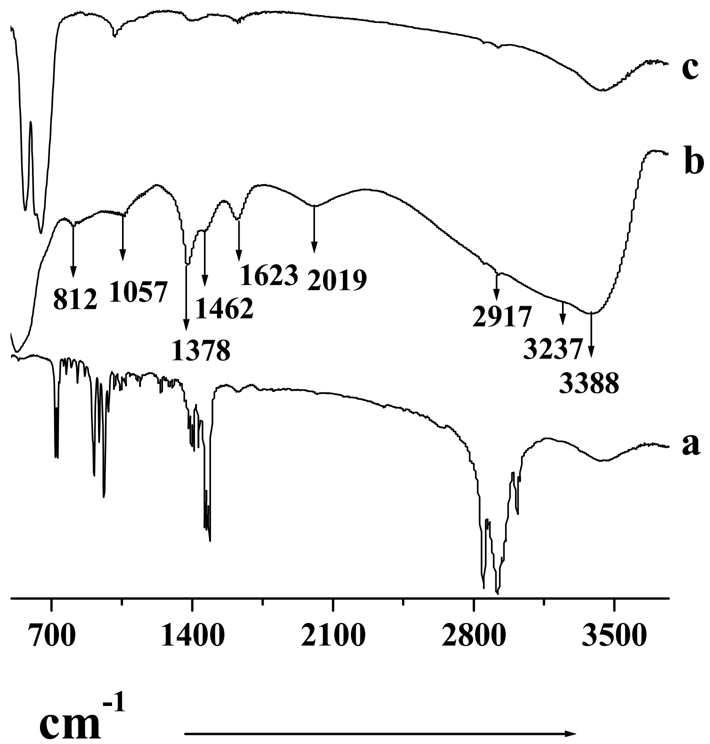

Figure 7. FTIR spectra of (a) pure CTAB (b) uncalcined and (c) calcined Cu-Cr sample.

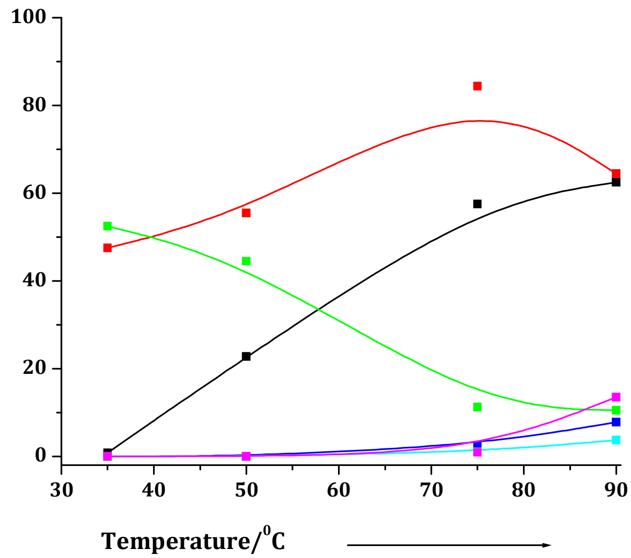

Fig. 8 Effect of temperature on toluene oxidation.
[■] Conversion of toluene; [●] Selectivity to benzaldehyde; [▲] Selectivity to benzyl alcohol; [▼]Selectivity to *p*-cresol; [♦]Selectivity to *o*-cresol; [◀]Selectivity to benzoic acid.
Reaction Condition: toluene =1g; Catalyst = 0.075g; toluene: H_2O_2 mole ratio =1:3; time= 10 h.

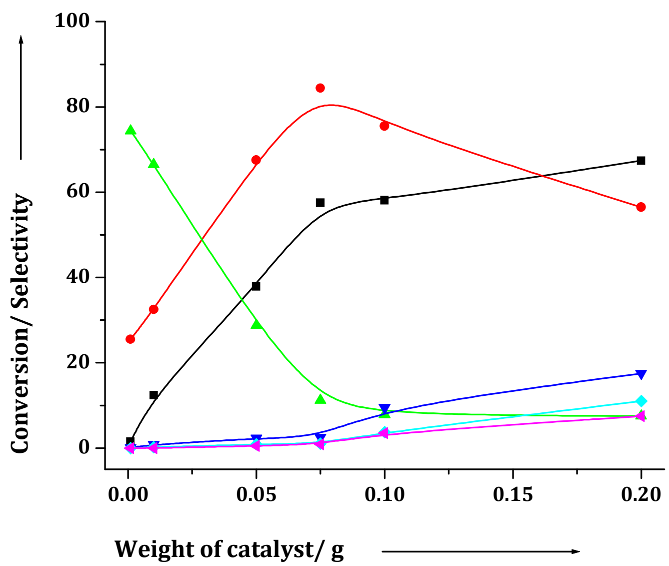

Fig. 9 Effect of catalyst weight on toluene oxidation.
[■] Conversion of toluene; [●] Selectivity to benzaldehyde; [▲] Selectivity to benzyl alcohol; [▼]Selectivity to *p*-cresol; [♦]Selectivity to *o*-cresol; [◀]Selectivity to benzoic acid.
Reaction Condition: toluene =1g; toluene: H_2O_2 mole ratio =1:3; temperature = 75°C; time= 10 h.

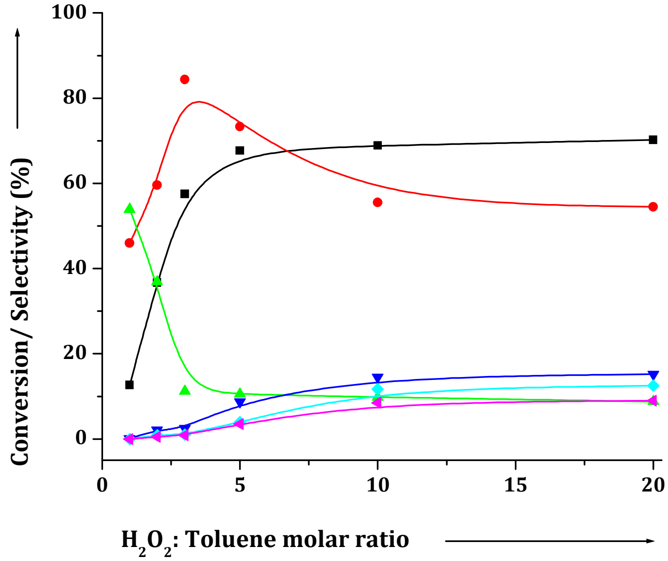

Fig. 10 Effect of toluene: H_2O_2 molar ratio on toluene oxidation.
[■] Conversion of toluene; [●] Selectivity to benzaldehyde; [▲] Selectivity to benzyl alcohol; [▼]Selectivity to *p*-cresol; [♦]Selectivity to *o*-cresol; [◀]Selectivity to benzoic acid.
Reaction Condition: toluene =1g; catalyst weight = 0.075 g; temperature = 75°C; time= 10 h.

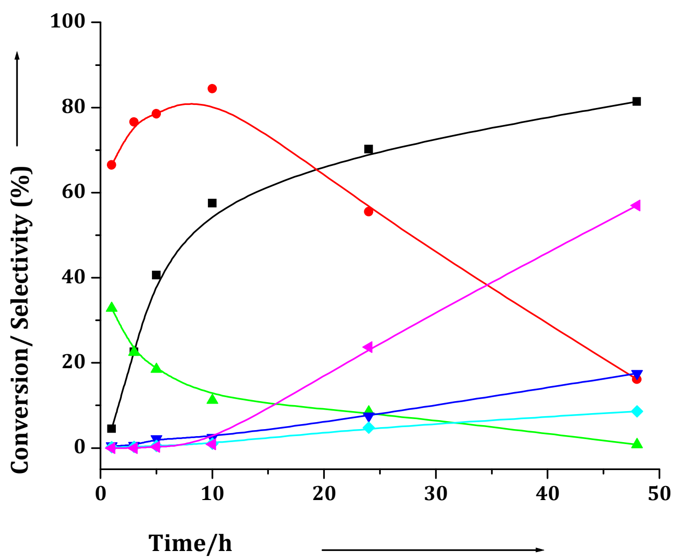

Fig. 11 Effect of time on stream on toluene oxidation.
[■] Conversion of toluene; [●] Selectivity to benzaldehyde; [▲] Selectivity to benzyl alcohol; [▼]Selectivity to *p*-cresol; [♦]Selectivity to *o*-cresol; [◀]Selectivity to benzoic acid.
Reaction Condition: toluene =1g; weight of catalyst = 0.075 g; toluene: H_2O_2 mole ratio =1:3; temperature = 75°C; time= 10 h.

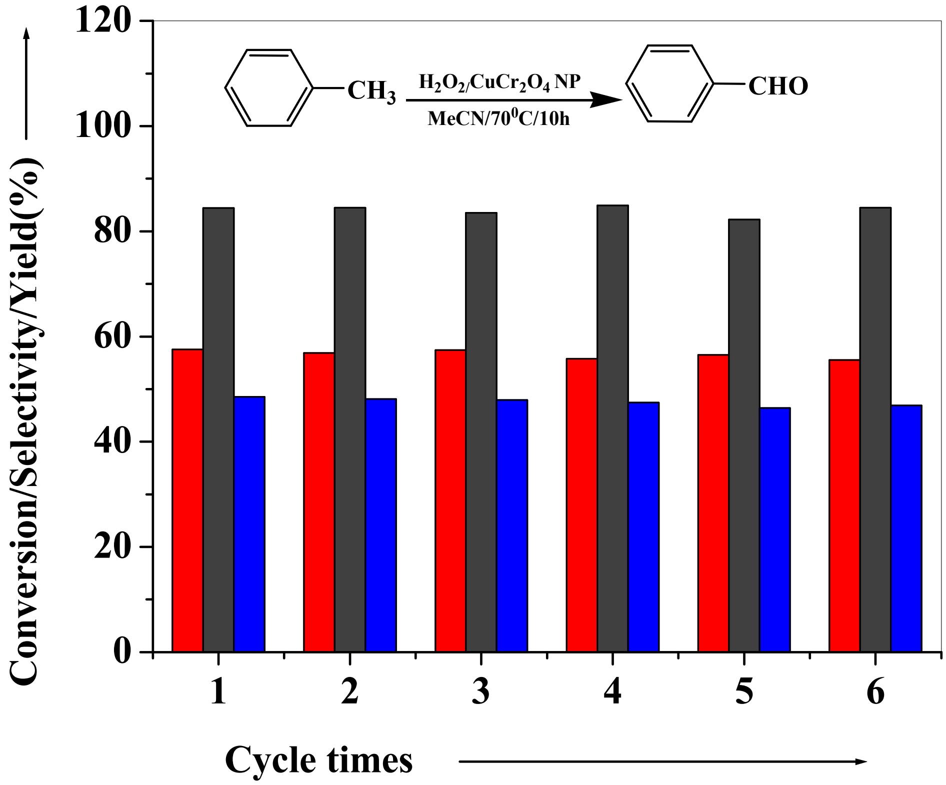

Fig. 12 Recyclability tests of $CuCr_2O_4$ spinel nanoparticles catalyst for the oxidation reaction of toluene to benzaldehyde.
[■] Conversion of toluene; [■] Selectivity to benzaldehyde; [■] Yield of benzaldehyde.

Table 1. Physicochemical properties of the $CuCr_2O_4$ catalyst

Entry	Catalyst	Cu/Cr[a] (mole ratio)	BET Surface Area (m^2/g)	Particle size (nm)	
				XRD[b]	TEM
1	$CuCr_2O_4$ (fresh)	0.5	92	28	40
2	$CuCr_2O_4$ (spent, after 5 recycle)	0.5	93	28.2	40

[a] Estimated by ICP-AES, [b] measured using Scherrer equation

Table 2. Summary of the EXAFS fitting results for Cu catalysts

Catalyst	Total path				Δk	ΔR	ΔE_0	R_f
	Path	R(10^{-1}nm)	CN	DW [$10^{-5}nm^2$]	[$10nm^{-1}$]	[$10nm^{-1}$]	[eV]	[%]
$CuCr_2O_4$ [Fresh catalyst]	Cu-O	1.938±0.078	2.5±0.4	3.6±0.9	3-14	1.0 -3.6	12.2±1	2.71
	Cu-O	1.886±0.023	4	13.0				
	Cu-O	3.140	4	17.0				
	Cu-Cr	3.245	4	7.3				
$CuCr_2O_4$ [Spent catalyst]	Cu-O	1.939±0.061	2.5±0.4	3.6±0.9	3-14	1.0 -3.6	12.2±0.9	2.03
	Cu-O	1.885±0.023	4	14.7				
	Cu-O	3.139	4	19.1				
	Cu-Cr	3.243	4	8.2				

Table 3 Activities of the different Cu-Cr[a]

Entry	Catalyst	Solvent	C_T[b] (%)	S_P[c] (%) Φ_{CHO} [Φ = Benzene Ring]	Φ_{CH2OH}	Others	Y_B[d] (%)
1.	CuO [COM]	MeCN	-	-	-	-	
2.	Cu_2O [COM]	MeCN	-	-	-	-	
3.	Cr_2O_3 [COM]	MeCN	-	-	-	-	
4.	$CuCr_2O_4$ [COM]	MeCN	6.6	55.5	11.5	33.0	3.6
5.	CuO-Cr_2O_3 [IMP]	MeCN	0.8	53.5	7.8	38.7	0.4
6.	Cu-Cr_2O_3[e]	MeCN	22.5	65.2	20.6	14.2	14.7
7.	CuO-Cr_2O_3 [CPM]	MeCN	1.2	50.2	14.3	35.5	0.6
8.	No Catalyst	MeCN	-	-	-	-	-
9.	$CuCr_2O_4$ NP	MeCN	57.5	84.4	11.2	4.4	48.5
10.	$CuCr_2O_4$ NP[f]	MeCN	55.5	84.5	13.4	2.1	46.8
11.	$CuCr_2O_4$ NP	AcOH	15.5	97.7	1.0	<1	15.1
12.	$CuCr_2O_4$ NP	DMF	1.8	55.5	10.5	34.0	0.9
13.	$CuCr_2O_4$ NP	DMSO	16.8	72.3	10.8	16.9	12.1
14.	$CuCr_2O_4$ NP	1,4-Dioxane	16.1	26.5	14.2	59.3	4.2
15.	$CuCr_2O_4$ NP	^{n}Octane	2.2	76.5	12.5	11.0	1.6

[a]Reaction conditions: solvent (acetonitrile) = 10ml, substrate (toluene) = 1g, $CuCr_2O_4$ nanoparticles catalyst = 0.075g, reaction temperature = 75 °C; time = 10 h; toluene: H_2O_2 mole ratio = 1: 2.5; [b]C_T: conversion of toluene based upon the FID-GC results= moles of toluene reacted/initial moles of toluene used] x 100; [c]S_P: selectivity of product calculated by total moles of product formed/total moles of toluene converted; [d]Y_B= conversion × selectivity/100; [e]Cu-nanoclusters supported on nanocrystalline Cr_2O_3; [f]catalyst after 5 reuse; COM= commercial; IMP = impregnation method; CPM= co-precipitation method; NP = nanoparticles